

RESEARCH ARTICLE

Classical nuclear motion: Does it fail to explain reactions and spectra in certain cases?

Erik Rohloff | Dominik A. Rudolph | Onno Strolka | Irmgard Frank 

Theoretical Chemistry, Leibniz University
Hannover, Hannover, Germany

Correspondence

Irmgard Frank, Theoretical Chemistry, Leibniz
University Hannover, Callinstr. 3A, 30167
Hannover, Germany.
Email: irmgard.frank@theochem.uni-hannover.de

Funding information

The study was supported by the Deutsche
Forschungsgemeinschaft (DFG), grant
FR1246/10-1.

Abstract

Is a classical description of nuclear motion sufficient when describing chemical reactions and spectra? This question is interesting because many researchers use a classical description of nuclear motion in molecular dynamics simulations. The present paper investigates some phenomena that were previously attributed to nuclear quantum effects. The question is if these phenomena can be modeled with traditional Car–Parrinello molecular dynamics, that is, with a method which treats nuclear motion classically and which is widely applied to the simulation of chemical reactions and spectra. We find that for the investigated system no additional paradigm is needed for describing chemical reactions. The special reactivity observed for carbenes can be attributed to the special environment represented by a noble gas matrix and to an additional transition state that was not considered before. Also the infrared spectrum of porphycene is perfectly modeled by traditional Car–Parrinello molecular dynamics. More studies are necessary to decide to what extent classical nuclear motion can replace the quantum mechanical description.

KEYWORDS

Car–Parrinello molecular dynamics, reaction mechanisms

1 | INTRODUCTION

Soon after the famous publication by Schrödinger it became clear, that, to make quantum chemical problems tractable, one should compute electronic structure and nuclear motion separately. To this end, the Born–Oppenheimer approximation was formulated. Within this approximation, the total wavefunction is described as a product of electronic and nuclear wavefunctions. Then, the electronic and nuclear problem are separated which leads to the electronic Hamilton operator. However, it turns out, that the nuclear–nuclear interaction must be added to the electronic energy if one wants to obtain what is called Born–Oppenheimer surfaces or also potential energy surfaces, PES. Hence, the only term which is not described in normal quantum chemical calculations, is the kinetic energy of the nuclei. That is, in normal quantum chemical calculations, instead of applying the Born–Oppenheimer approximation in its original version, we describe the situation at zero Kelvin. What is left for the nuclei? Car and Parrinello gave an answer with their extended Lagrangian [1]. They describe the electronic cloud with the density functional approximation and the nuclear motion with classical Newton theory. With this ingenious approach it became possible to simulate chemical reactions at finite temperature at the ab-initio level of theory [2, 3]. The temperature is reflected by a Maxwell–Boltzmann distribution of atomic

Research Resources: Part of the calculations were performed on the local cluster of the Leibniz University of Hannover at the LUIS and on the Höchstleistungsrechner Nord, HLRN, maintained by the North German Supercomputing Alliance, project nic00061.

This is an open access article under the terms of the [Creative Commons Attribution](https://creativecommons.org/licenses/by/4.0/) License, which permits use, distribution and reproduction in any medium, provided the original work is properly cited.

© 2022 The Authors. *International Journal of Quantum Chemistry* published by Wiley Periodicals LLC.

velocities, which develops quickly in molecular dynamics simulations, because it is the most likely distribution. Car and Parrinello also proposed to introduce a quasi-classical treatment of the electrons. The present considerations concerning nuclear motion are essentially independent on the description of electronic motion with Car–Parrinello molecular dynamics or, alternatively, Born–Oppenheimer molecular dynamics, where the system is quenched to the Born–Oppenheimer surface in every step. The Car–Parrinello picture of electronic motion is just more elegant.

Classical nuclear motion was certainly introduced as an approximation to quantum nuclear motion. The question is what differences to experiment are caused by a classical treatment of nuclear motion. In particular, one might ask if it is possible to describe reliably chemical reactions and vibrational spectra in this way or if there are pitfalls. This is interesting because many authors use the classical approach for nuclear motion, not only in pure QM but also in QM/MM calculations (see e.g., References [4, 5]). Also the computation of infrared spectra from molecular dynamics simulations has been performed since many years [6, 7].

Nevertheless, two examples have been published recently with the intention to prove the necessity of quantum mechanical nuclear motion: The isomerization of carbenes [8, 9] and the infrared spectrum of porphycene [10, 11]. In the present paper we investigate these phenomena using the classical part of the Car–Parrinello molecular dynamics code.

2 | RESULTS AND DISCUSSION

2.1 | Isomerization of methylhydroxycarbene

Schreiner et al. [8, 9] investigated a highly interesting reaction, namely the isomerization of carbenes, in particular the isomerization of methylhydroxycarbene **1**. This compound can in principle undergo the thermal isomerization to acetaldehyde **2** via transition state **TS1** or to vinyl alcohol **3** via transition state **TS2** (see Figure 1). Experimentally, at low temperatures the more stable product **2** is observed, even if the reaction barrier is higher than that for the reaction to product **3**.

On this basis, Schreiner introduced a third reactivity paradigm besides thermodynamic or kinetic control. He attributed the observation of **2** to nuclear tunneling through the narrower barrier. This explanation is not convincing because the width of a barrier is not well-defined in contrast to the height of a barrier. The latter one has the unit of an energy and corresponds to a difference of state functions. In contrast, the width of a barrier may be a combination of parameters like bond distances, angles, etc. In three-dimensional space, it is not well-defined.

If an expected product is not observed, this may have several reasons, including an alternative decomposition. In such a situation, Car–Parrinello molecular dynamics may be helpful. What do we find, if we investigate the reactions of methylhydroxycarbene using Car–Parrinello molecular dynamics simulations? First, it has to be emphasized that we cannot simulate the full reaction, this would take quadrillions of CPU hours. We must accelerate the reactions in some way. As we do not want to restrict the reaction pathway to certain degrees of freedom, we can get an acceleration only by raising the temperature. Of course this is not the same as simulating the full reaction at low temperatures, but we can get some information about possible reaction pathways that might have been overlooked. The result is summarized in Table 1. We did simulations with initial kinetic energies ranging from 2000 to 10 000 K. Additional suites of simulations with a longer simulation time and a larger simulation cell were performed to check these results (see Supporting information). We performed simulations for the two isomers of methylhydroxycarbene, **1** and **1a**. **1** and **1a** reacted in a similar way. At high temperatures, the reaction to both compounds **2** and **3** is

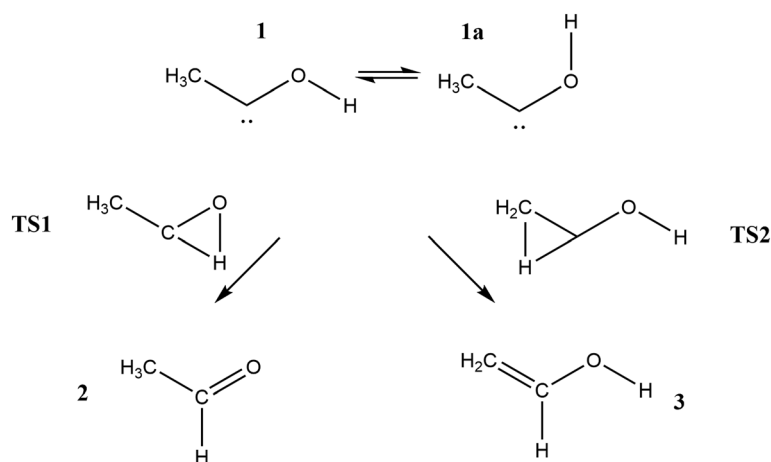


FIGURE 1 Reactions starting from methylhydroxycarbene **1** as discussed in References [8, 9]. Experimentally, acetaldehyde **2** is formed

TABLE 1 Protocol of the CPMD simulations

Isomer	Argon atoms	Temperature (K)	Intermediate	Time (ps)	Final product	Time (ps)
1	0	2000	-	-	-	-
1	0	4000	-	-	-	-
1	0	6000	-	-	-	-
1	0	8000	3	0.71	H ₂ O	0.84
1	0	10 000	2	0.09	CO	0.10
1	24	2000	-	-	-	-
1	24	4000	-	-	2	0.39
1	24	6000	-	-	3	0.39
1	24	8000	-	-	CO	0.35
1	24	10 000	2	0.22	H ₂	0.34
1	32	2000	-	-	-	-
1	32	4000	-	-	-	-
1	32	6000	-	-	2	0.44
1	32	8000	3	0.17	2	0.67
1	32	10 000	3	0.19	H ₂	0.22
1	40	2000	-	-	2	0.81
1	40	4000	-	-	3	0.22
1	40	6000	3	0.20	2	0.59
1	40	8000	3	0.02	2	2.37
1	40	10 000	-	-	H ₂	0.77
1a	0	2000	-	-	-	-
1a	0	4000	-	-	-	-
1a	0	6000	-	-	CO	0.34
1a	0	8000	-	-	CO	0.33
1a	0	10 000	-	-	CO	0.31
1a	24	2000	-	-	-	-
1a	24	4000	-	-	-	-
1a	24	6000	3	0.26	H ₂	0.56
1a	24	8000	-	-	3	0.06
1a	24	10 000	3	0.01	H ₂ O	0.40
1a	32	2000	-	-	-	-
1a	32	4000	-	-	3	2.04
1a	32	6000	-	-	H ₂	0.43
1a	32	8000	-	-	3	0.03
1a	32	10 000	3	0.02	H ₂	0.14
1a	40	2000	-	-	2	0.45
1a	40	4000	-	-	2	0.82
1a	40	6000	H ₂ O	0.17	3	0.65
1a	40	8000	-	-	3	0.20
1a	40	10 000	3	0.05	2	0.28

Note: The total simulation time of every run was 2.66 ps. The most relevant products are specified. Products **2** and **3** are formed in an approximately equal amount. Hereby, compound **3** is often converted to **2**. Formation of H₂O, CO or H₂ means complete decomposition. For simulations with a larger unit cell and longer simulation times (see Supporting information).

observed. Several aspects are striking: **3** can be converted into the thermodynamic product **2** via a four-membered-ring transition state **TS3** (see Figures 2 and 3). Furthermore, increasing the argon pressure leads to a more efficient formation of **2**. Finally, decomposition to products like CO, H₂, and H₂O is observed. In the gas phase and at high temperatures, the decomposition is predominant.

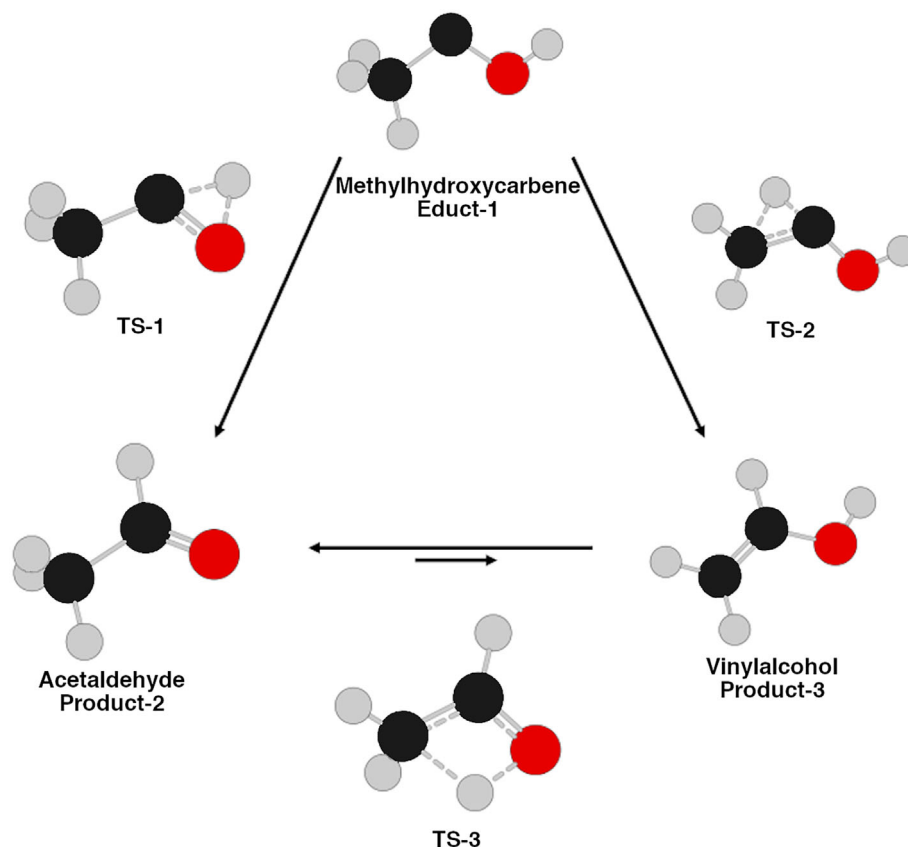


FIGURE 2 Sketch of the reactions starting from methylhydroxycarbene **1**. In addition to transition states **TS1** and **TS2** there is yet another transition state **TS3** which explains the experimental observations

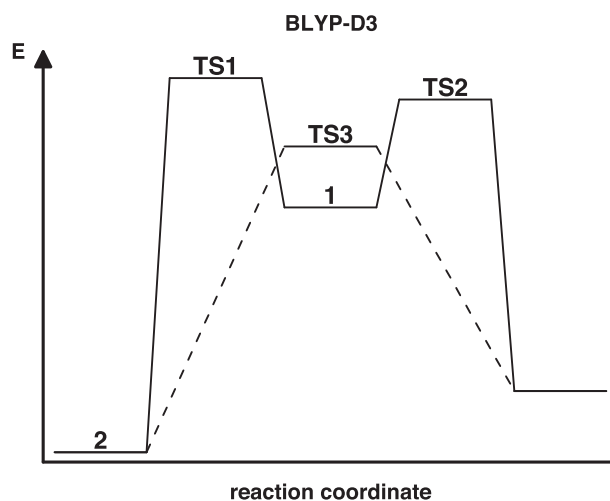


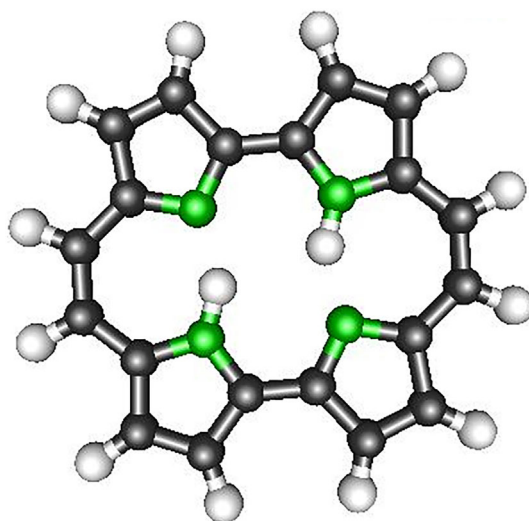
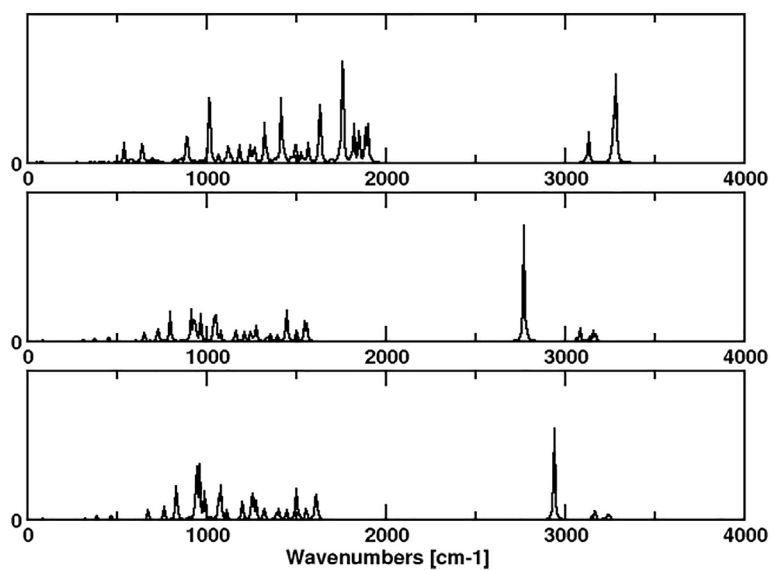
FIGURE 3 Sketch of the energetics of the reactions starting from methylhydroxycarbene **1**. Via transition state **TS3** the thermodynamic product **2** can be formed

The latter observation is due to the exothermicity of the reactions. A high amount of potential energy is converted into kinetic energy which leads to decomposition. This is different if the molecules are environed by an argon matrix. The matrix forms kind of a nanoreactor as it was introduced by Martinez [12]. By using the CPMD code, we are employing a different concept to realizing such a nanoreactor, namely periodic boundary conditions and an explicit solvent or environment. The effect is the same: The reactive species is contained in a small space, the atoms can hardly escape on the timescale of the reaction. At the same time, kinetic energy is transferred to the environment, respectively, the matrix, thus preventing thermal decomposition.

TABLE 2 Energetics (in kcal/mol) as computed with Gaussian

Comp.	BLYP	B3LYP	BLYP-D3	B3LYP-D3	HF	MP2	CCSD(T)	B2PLYP	B2PLYP-D3
1	52.1	51.6	52.4	52.0	47.6	54.9	51.2	52.6	52.7
2	0.0	0.0	0.0	0.0	0.0	0.0	0.0	0.0	0.0
3	12.9	12.5	13.1	12.8	14.6	14.6	14.1	13.7	13.8
TS1	79.8	83.7	80.1	84.0	97.2	84.4	82.7	83.8	84.0
TS2	75.3	76.6	75.5	76.8	83.3	80.1	78.4	78.2	78.3
TS3	65.3	69.5	65.5	69.7	86.9	71.0	72.6	70.6	70.6

Note: All methods agree reasonable well. The largest deviations are obtained with Hartree-Fock.

**FIGURE 4** Porphycene**FIGURE 5** Infrared spectra of porphycene computed with Gaussian (at zero Kelvin). From top to bottom: AM1, BLYP, B3LYP

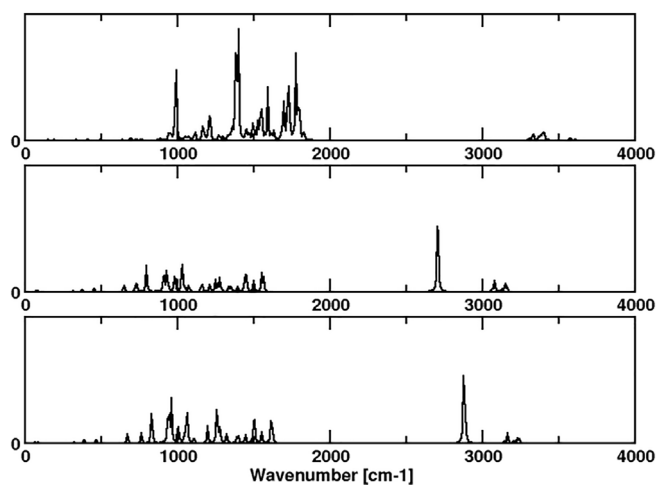


FIGURE 6 Infrared spectra of porphycene computed with Gaussian (at zero Kelvin). From top to bottom: HF, BLYP-D, B3LYP-D

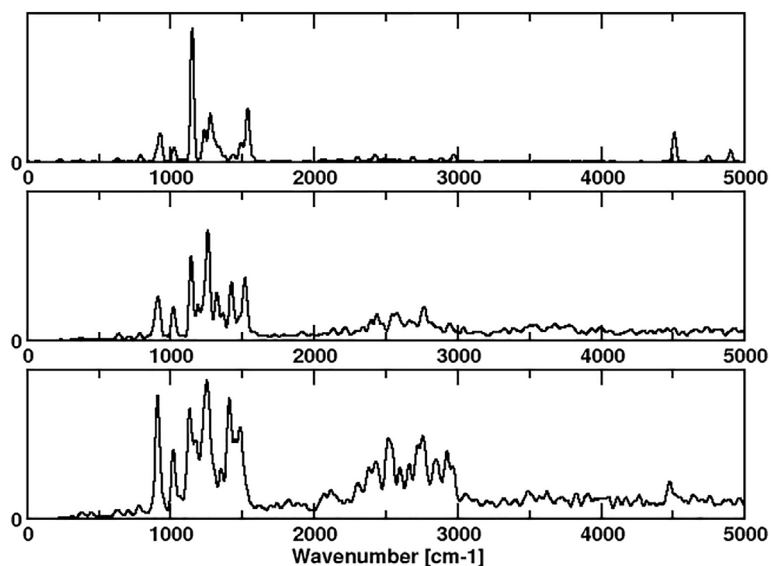


FIGURE 7 Infrared spectra of porphycene computed with CPMD/BLYP and TRAVIS. From top to bottom: 10 K, 290 K, 550 K. the spectrum at 290 K fits best to experiment

Finally, the transition state **TS3** explains why only the thermodynamic product is observed in experiment. In our simulations, an equal amount of **2** and **3** is formed in the end whereby one of the reaction pathways is $1/1a \rightarrow 3 \rightarrow 2$. Already on the picosecond time scale, this reaction pathway shifts the result strongly in the direction of **2**. On experimental time scales this will lead nearly exclusively to the formation of **2** in an amount determined by the energy difference between **2** and **3**, that is, the thermodynamical product will be obtained predominantly. This result which was obtained by CPMD simulations at very high temperatures, was confirmed by static calculations up to the CCSD(T) level (Table 2).

2.2 | Infrared spectrum of porphycene

Rossi and coworkers [10] investigated the infrared spectrum of porphycene (Figure 4).

They attributed a feature at about 2500 cm^{-1} to a quantum mechanical nuclear motion. We did several calculations to elucidate this phenomenon. We started from static calculations performed with the Gaussian program package (Figures 5 and 6). The first observation is, that there is certainly no agreement within 50 cm^{-1} , the error of the electronic structure methods is larger. The dispersion correction has only a minor influence. The experimental absorption around 2500 cm^{-1} is missing completely in the calculations. All methods agree in this point.

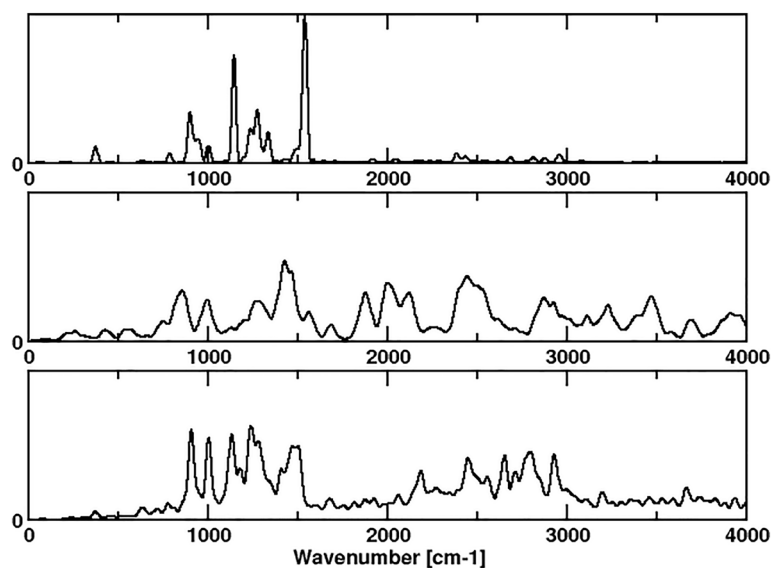


FIGURE 8 Infrared spectra of porphycene computed with CPMD/BLYP-D and TRAVIS. From top to bottom: 10 K, 280 K, 550 K

This changes, if temperature is applied in a Car-Parrinello molecular dynamics simulation (Figures 7 and 8). Figure 7 displays the results without dispersion correction, Figure 8 is with dispersion correction. At 10 K, there is only weak absorption in the region between 2000 and 3000 cm^{-1} . This changes strongly, if the temperature is raised. In the simulation at 290 K without dispersion correction we get a pattern which agrees best with the experiment (see figure 4d in Reference [13]). We observe that the agreement of electronic structure methods with experiment is a bit accidental, while the application of temperature can be essential.

3 | CONCLUSIONS

We have simulated phenomena that were recently reported with the intention to prove that quantum mechanical nuclear motion is necessary to explain them. We find alternative explanations for the observations.

The experimentally observed reaction of methylhydroxycarbene **1** to acetaldehyde **2** is readily explained by an additional transition state for the reaction route $\mathbf{1} \rightarrow \mathbf{3} \rightarrow \mathbf{2}$. The thermodynamical product is formed efficiently in this way. On the experimental time scale a distribution according to the energy difference of the products is obtained. As a result, **2** is the dominating product. An important parameter is the argon matrix. The higher the argon pressure, the more likely is the formation of **2**. Without a surrounding matrix, the decomposition to a variety of products is dominant at high energies. Hereby, the matrix has two effects, namely keeping the atoms together and taking up the energy which is set free in these exothermic reactions. The simulations show the reaction to the experimentally observed thermodynamical product. An additional paradigm is not needed. At this point, however, also the short-comings of our approach should be emphasized: The computations performed at extremely high temperatures may not reproduce the behavior of the carbene at normal temperatures. Also we are restricted to the BLYP functional if we want to perform longer simulation runs. Hence, the method comparison is important: By good luck we find in static calculations up to the CCSD(T) level that there is little method dependency in this system.

The picture is essentially the same for the infrared spectrum of porphycene. It is obvious that for medium-sized molecules the computation of accurate infrared spectra is problematic. This is primarily due to the lack of thermal motion in static quantum chemical calculations and to the lack of accuracy of the electronic structure methods. It is obvious that application of temperature, as it is possible in a molecular dynamics simulation, represents a clear improvement. The application of path-integral calculations has a similar effect. Also in this case it is possible to explain the experimental observations without advocating quantum effects in nuclear motion. Temperature can play a major role for computing infrared spectra.

To conclude, a clear deviation from experiment caused by the neglect of quantum effects in nuclear motion is missing for the two systems under investigation. Thanks to the fact that we have a Maxwell-Boltzmann distribution of velocities in our many-body simulations, a clear difference to experiment like an ultraviolet catastrophe or a classically forbidden region does not appear [14]. Further computations are necessary to understand the limitations of a classical description of nuclear motion.

4 | METHODS

Car–Parrinello molecular dynamics simulations [1, 3, 15] have been performed in the NVE ensemble using the Becke–Lee–Yang–Parr (BLYP) functional in connection with the Grimme dispersion correction [16]. In the case of the carbene isomerization, the time step was chosen as 1 a.u. (0.024 fs) and the fictitious electron mass as 100 a.u. This relatively small time step is needed for describing the high-temperature scenario accurately. Troullier–Martins pseudopotentials as optimized for the BLYP functional were employed for describing the core electrons [4, 17]. For the reactive simulations, the spin-unrestricted version of Kohn–Sham theory was employed [18]. The plane-wave cutoff which determines the size of the basis set, was set to 70.0 Rydberg. The simulation cell size was $16 \times 16 \times 16$ a.u.³ ($8.5 \times 8.5 \times 8.5$ Å³). Argon matrices with different densities were created: gas phase (0 argon atoms), low pressure (24 argon atoms), normal pressure (32 argon atoms), high pressure (40 argon atoms). After equilibration of stable, neutral closed-shell systems, the initial temperature was set to 2000, 4000, 6000, 8000, and 10 000 K. During the production runs, the temperature was not controlled. A list with the different simulation protocols is contained in Table 1.

These results were checked in two different ways:

First, by determination of the relevant minima and transition states with the Gaussian program package [19]. These were performed using BLYP, B3LYP, BLYP-D3, B3LYP-D3, Hartree–Fock, MP2, CCSD(T), B2PLYP, and B2PLYP-D3 [16, 19–22]. The basis set was chosen to be 6-311G(d,p).

In addition, several additional suites of simulations were performed using CPU time at the supercomputer HLRN. They are summarized in the Supporting information. First, a larger unit cell ($20 \times 20 \times 20$ a.u.³/ $10.6 \times 10.6 \times 10.6$ Å³) was used. To avoid sudden jumps in energy after the equilibration, simulated annealing was employed using heating factors of 1.0001 and 1.00001. In addition, the triplet reaction was investigated for comparison. Finally, prolonged simulations were performed at lower temperatures (see Supporting information). All these additional simulations resulted in no additional reaction pathways.

In the case of porphycene, a time step of 5 a.u. (0.12 fs) and a fictitious electron mass of 400 a.u. was chosen which was sufficient to get stable simulations at normal energies. The plane-wave cutoff was set to 50.0 Rydberg, as the system contains no problematic atoms. The simulation cell size was $24 \times 24 \times 24$ a.u.³ ($12.7 \times 12.7 \times 12.7$ Å³) to allow for free rotation. Porphycene was optimized, then the TEMPERATURE IONS option was used to set the start energy to 6, 600, and 1200 K, respectively. As more or less half of the energy is converted into potential energy, this resulted in temperatures of about 10, 290, and 550 K. During the production runs, the temperature was not controlled. Wannier centers were computed using the DIPOLE DYNAMICS keyword. The TRAVIS program [7] was used to compute the spectra from the trajectories.

For comparison, frequency calculations with the Gaussian program package [19] were performed using AM1, Hartree–Fock, BLYP, B3LYP, BLYP-D, and B3LYP-D [19–21, 23, 24]. The basis set was chosen to be 6-311G(d,p).

ACKNOWLEDGMENT

Open access funding enabled and organized by Projekt DEAL.

AUTHOR CONTRIBUTIONS

Irmgard Frank: Conceptualization; funding acquisition; investigation; methodology; project administration; supervision; writing – original draft. **Erik Rohloff:** Data curation; formal analysis; investigation; validation; visualization; writing – review and editing. **Dominik A. Rudolph:** Data curation; formal analysis; investigation; validation; visualization; writing – review and editing. **Onno Strolka:** Data curation; formal analysis; investigation; validation; visualization; writing – review and editing.

DATA AVAILABILITY STATEMENT

CPMD input files are available on demand from the corresponding author.

ORCID

Irmgard Frank  <https://orcid.org/0000-0001-9871-5183>

REFERENCES

- [1] R. Car, M. Parrinello, *Phys. Rev. Lett.* **1985**, 55, 2471.
- [2] M. Parrinello, *J. Solid State Chem.* **1997**, 102, 107.
- [3] D. Marx, J. Hutter, *Ab Initio Molecular Dynamics: Basic Theory and Advanced Methods*, Cambridge University Press, Cambridge **2009**.
- [4] M. Boero, M. Parrinello, K. Terakura, H. Weiss, *Mol. Phys.* **2002**, 100, 2935.
- [5] U. Röhrig, L. Guidoni, A. Laio, I. Frank, U. Röthlisberger, *J. Am. Chem. Soc.* **2004**, 126, 15328.
- [6] P. L. Silvestrelli, M. Bernasconi, M. Parrinello, *Chem. Phys. Lett.* **1997**, 277, 478.
- [7] M. Thomas, M. Brehm, R. Fligg, P. Vöhringer, B. Kirchner, *Phys. Chem. Chem. Phys.* **2013**, 15, 6608.
- [8] P. R. Schreiner, H. P. Reisenauer, D. Ley, D. Gerbig, C.-H. Wu, W. D. Allen, *Science* **2011**, 332, 1300.
- [9] P. R. Schreiner, *J. Am. Chem. Soc.* **2017**, 139, 15276.

- [10] Y. Litman, J. O. Richardson, T. Kumagai, M. Rossi, *J. Am. Chem. Soc.* **2019**, *141*, 2526.
- [11] S. Gawinkowski, L. Walewski, A. Vdovin, A. Slenczka, S. Rols, M. R. Johnson, B. Lesyng, J. Waluk, *Phys. Chem. Chem. Phys.* **2012**, *14*, 5489.
- [12] L.-P. Wang, A. Titov, R. McGibbon, F. Liu, V. S. Pande, T. J. Martinez, *Nat. Chem.* **2014**, *6*, 1044.
- [13] Y. Litman, D. Donadio, M. Ceriotti, M. Rossi, *J. Chem. Phys.* **2018**, *148*, 102320.
- [14] R. C. Büchel, D. A. Rudolph, I. Frank, *Int. J. Quantum Chem.* **2021**, *121*, e26555.
- [15] Version 4.1, J. Hutter et al., Copyright IBM Corp 1990–2015, Copyright MPI für Festkörperforschung Stuttgart 1997–2001. <http://www.cpmc.org/>.
- [16] S. Grimme, *J. Comput. Chem.* **2006**, *27*, 1787.
- [17] N. Troullier, J. L. Martins, *Phys. Rev. B* **1993**, *1991*, 43.
- [18] O. Gunnarsson, B. I. Lundqvist, *Phys. Rev. B* **1976**, *13*, 4274.
- [19] M. J. Frisch, G. W. Trucks, H. B. Schlegel, G. E. Scuseria, M. A. Robb, J. R. Cheeseman, G. Scalmani, V. Barone, G. A. Petersson, H. Nakatsuji, X. Li, M. Caricato, A. V. Marenich, J. Bloino, B. G. Janesko, R. Gomperts, B. Mennucci, H. P. Hratchian, J. V. Ortiz, A. F. Izmaylov, J. L. Sonnenberg, D. Williams-Young, F. Ding, F. Lipparini, F. Egidi, J. Goings, B. Peng, A. Petrone, T. Henderson, D. Ranasinghe, V. G. Zakrzewski, J. Gao, N. Rega, G. Zheng, W. Liang, M. Hada, M. Ehara, K. Toyota, R. Fukuda, J. Hasegawa, M. Ishida, T. Nakajima, Y. Honda, O. Kitao, H. Nakai, T. Vreven, K. Throssell, J. A. Montgomery Jr., J. E. Peralta, F. Ogliaro, M. J. Bearpark, J. J. Heyd, E. N. Brothers, K. N. Kudin, V. N. Staroverov, T. A. Keith, R. Kobayashi, J. Normand, K. Raghavachari, A. P. Rendell, J. C. Burant, S. S. Iyengar, J. Tomasi, M. Cossi, J. M. Millam, M. Klene, C. Adamo, R. Cammi, J. W. Ochterski, R. L. Martin, K. Morokuma, O. Farkas, J. B. Foresman, D. J. Fox, *Gaussian16 Revision A.03*, Gaussian Inc., Wallingford CT, United States **2016**.
- [20] A. Becke, *Phys. Rev. A* **1988**, *38*, 3098.
- [21] A. Becke, *J. Chem. Phys.* **1993**, *98*, 1372.
- [22] S. Grimme, *J. Chem. Phys.* **2006**, *124*, 034108.
- [23] M. J. S. Dewar, E. G. Zoebisch, E. F. Healy, J. J. P. Stewart, *J. Am. Chem. Soc.* **1985**, *107*, 3902.
- [24] S. Grimme, *J. Comput. Chem.* **2004**, *25*, 1463.

SUPPORTING INFORMATION

Additional supporting information may be found in the online version of the article at the publisher's website.

How to cite this article: E. Rohloff, D. A. Rudolph, O. Strolka, I. Frank, *Int. J. Quantum Chem.* **2022**, *122*(12), e26902. <https://doi.org/10.1002/qua.26902>